A Capacitor Modeling Method for Integrated Magnetic Components in DC/DC Converters

Liang Yan, *Member, IEEE,* and Brad Lehman, *Member, IEEE*

***Abstract*—For the special case of dc/dc converters, the gyrator-capacitor model is revised by replacing gyrators with current sources to symbolize the electrical actions on windings. The revised capacitor model is suitable for analyzing integrated magnetic components. Several examples illustrate the usage of this approach. Comparisons between the revised capacitor model and the conventional reluctance model for magnetic calculation and integration are presented.**

***Index Terms*—Gyrators, integrated magnetics, modeling, windings.**

I. Introduction

DC/DC converters with integrated magnetics have seen widespread applications [1], [2], due to their potential size reduction from combining inductors and transformers into one magnetic assembly. Additionally, some topologies with integrated magnetics have special qualities not found in their counterparts with discrete magnetic cores, such as the ability to lower current ripple or reduce voltage stress [3]. These superior characteristics instigate the study of modeling and design techniques for integrated magnetic components.

Several magnetic modeling techniques are available for integrated magnetic components. The conventional reluctance model [4]–[7] is the well-known approach. It is based on magnetomotive force (mmf)-voltage and flux-current analogies. The reluctance of a magnetic core section is analogous to a resistor; and a winding is represented by a voltage source. The magnetic circuit can then be modeled by its electrical equivalent to derive design parameters such as flux densities, gap lengths, etc. A variation of this approach uses current sources instead of voltage sources to represent windings in order to simplify the model for coupled inductors and improve simulation speed [8].

Another approach is the gyrator-capacitor modeling method. In the late 1960s, the gyrator-capacitor model was proposed by using a different set of analogies: mmf-voltage and flux rate (i.e., the differential of flux)-current [9]–[11]. In the magnetic circuit, the permeance of a magnetic core section is analogous to a capacitor. A gyrator represents a winding. The gyrator is an electrical-magnetic interface that links the electrical circuit and the magnetic circuit. The gyrator-capacitor model has several advantages over the conventional reluctance model. For example, the capacitor can store electrical energy. This gives insight into the physical meanings of magnetic energy, as explained by Hamill in [12] and [13]. Therefore, several recent publications have advocated the gyrator-capacitor modeling method for magnetic design [12]–[16].

To date the gyrator-capacitor model is mainly advocated as a simulation tool that includes both electrical and magnetic circuits in one simulation environment. Although this model offers better understanding of magnetic components, it has not become a popular method for design and calculation. Actually, for the design and calculation of magnetic components, a complete electrical-magnetic modeling structure is not necessary. For example, the reluctance model symbolizes the electrical actions on windings as voltage sources and removes the electrical part altogether. The simple reluctance model structure makes it possible to easily analyze magnetic core properties in terms of Kirchoff's Voltage Law (KVL) and Kirchoff's Current Law (KCL). Thus, the reluctance modeling method is popular among design engineers. The gyrator-capacitor modeling method [9]–[16], on the other hand, is primarily used as a simulation tool and it does not yet have a simplified circuit model that can be used by power supply designers.

The purpose of this paper is to further promote the capacitor modeling method for the magnetic design. That is, this paper extends and simplifies the gyrator-capacitor modeling approach for typical integrated magnetic converters to show that it can be used as a simple and effective analysis and design method. Since it does not focus on the circuit simulation, the gyrators and the electrical part can be removed. (Hence, we call it a "capacitor model".) Under certain assumptions, the capacitor model provides more design convenience than the conventional reluctance model, particularly for dc/dc converters with integrated magnetics. In summary, this paper

- applies a simplified capacitor modeling approach to magnetic analysis, calculation and integration;
- proposes and justifies the use of current sources to symbolize the electrical actions on windings instead of gyrators, for dc/dc converters under periodic steady state operation;
- demonstrates the following advantages of the modeling approach over the conventional reluctance model on magnetic design:
  - —simplified calculation of voltage-related parameters such as input-to-output voltage ratio, flux swing in the core, etc.;
  - —simplified calculation of current ripple for complicated magnetic assemblies;
  - —direct integration of magnetic components.

In Section II, the reluctance model and the gyrator-capacitor model are reviewed by using an integrated magnetic forward

Manuscript received November 11, 2003; revised December 7, 2004. This paper appeared in the IEEE Power Electronics Specialists Conference; Vancouver, CA, 2001. Recommended by Associate Editor C. R. Sullivan.

The authors are with the Department of Electrical and Computer Engineering, Northeastern University, Boston, MA 02115 USA (e-mail: liang_yan@mksinst.com; lehman@ece.neu.edu).

Digital Object Identifier 10.1109/TPEL.2005.854018

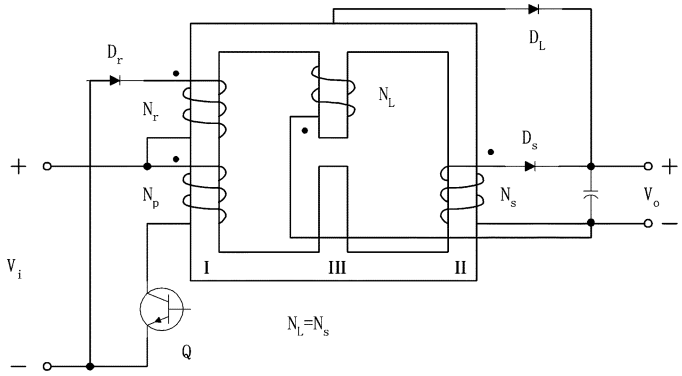

Fig. 1. Integrated magnetic forward converter [2].

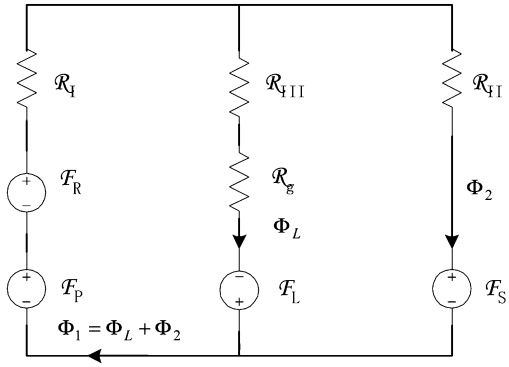

Fig. 2. Resistor model of the forward converter in Fig. 1 [2].

converter as an example. Section III proposes a simplified capacitor model and justifies the proposed simplifications. Section IV presents differences between the capacitor model and the reluctance model when the models are used to calculate magnetic quantities. Section V presents their differences when modeling magnetic integration. Section VI gives conclusions.

II. Brief Review of Known Modeling Methods

This section briefly reviews the reluctance model [4]–[7] and the gyrator-capacitor [9]–[13] model. An integrated magnetic forward converter in Fig. 1 is used as an example to create the models. These models will be frequently referred to in the following sections for comparisons with the revised capacitor model that is proposed in Section III. Advantages and disadvantages of the reluctance and the gyrator-capacitor model, as well as the reasons to modify the gyrator-capacitor model, are discussed in this section.

A. Reluctance Model

In practice, the reluctance model is created from observation of the physical geometry and the winding locations of a real magnetic assembly. Magnetic core legs and gaps are modeled as resistors with the resistance equal to their corresponding reluctance. Windings are replaced by voltage sources.

As an example, the reluctance model of the integrated magnetic forward converter in Fig. 1 is shown in Fig. 2 [2]. Here, Φ is the flux rate; $\mathcal{F}$ is the magnetomotive force (mmf) and $\mathcal{R}$ is the reluctance. According to the well known "right-hand-rule," the active windings (i.e., the windings that are conducting current) can be found in each operating state. Fig. 3(a)–(c) presents the models in three operating states. In each state, the currents determine the mmfs of the windings. The mmfs of the reluctance are calculated by KVL. Hence, flux densities in three core legs can be derived.

To analyze the electrical circuit, a duality transformation is performed to generate the inductor model in Fig. 4. In the inductor model, the windings are mapped to coupled-inductors. The model in Fig. 4 can be further simplified to a familiar discrete core forward converter of Fig. 5 under conditions $N_L = N_s$ and $L_c \gg L_g$, where L_c is the equivalent core inductance and L_g is the equivalent gap inductance.

B. Gyrator-Capacitor Approach

In the gyrator-capacitor model [12], core legs and gaps are modeled by capacitors with capacitance equal to their corresponding permeance. Fig. 6(a) shows the gyrator-capacitor model of the integrated magnetic forward converter in Fig. 1, where $\mathcal{P}_{I-III}$ are the permeances of three core legs and $\mathcal{P}_g$ is the permeance of the gap. Four gyrators G_p, G_r, G_L, and G_s represent four windings, respectively.

Each gyrator describes the following mathematical relationship: $\dot{\Phi} = V/N$ and $\mathcal{F} = NI$ as in Fig. 6(b). Here, $\dot{\Phi}$ is the flux rate enclosed by a winding that supports a voltage V; $\mathcal{F}$ is the mmf of the winding with current I and N is the number of winding turns. Once the circuit model of the magnetic assembly is established, KCL and KVL (which are based on Gauss' law and Ampere's law, respectively) can be used to calculate the magnetic quantities.

Unlike the conventional method that separates the reluctance model and its inductor equivalent, the gyrator-capacitor model includes both the magnetic circuit and the electrical circuit. Using current controlled voltage sources to represent the gyrators, the entire circuit can be easily simulated in SPICE by using the circuit in Fig. 6 [12]–[16].

C. Comments

The reluctance model maintains the physical topologies of magnetic components and removes the electrical parts. The compact model structure can help to establish the concept of magnetic quantities. However, this model does not include an important parameter—flux rate. Therefore, it cannot directly analyze or solve problems regarding flux change, voltage stress, etc. To illustrate this difficulty, consider the circuit in Fig. 1. In order to determine the voltage rating of diode D_L, it is necessary to obtain the voltage on winding N_L when switch Q is closed. This voltage cannot be directly derived from the reluctance model in Fig. 3(a). It is typically calculated in its inductor model of Fig. 4.

The gyrator-capacitor model is also a circuit model that can be used to obtain the magnetic quantities. Thanks to its special flow variable, flux rate $\dot{\Phi}$, instantaneous voltage on the winding is simply $V = \dot{\Phi}N$. However, compared to the reluctance model, the circuit model in Fig. 6(a) is not concise. Perhaps due to the gyrators and the electrical circuit in the model, designers tend to utilize the gyrator-capacitor model as a simulation tool instead of a competent analysis method. As a result, its

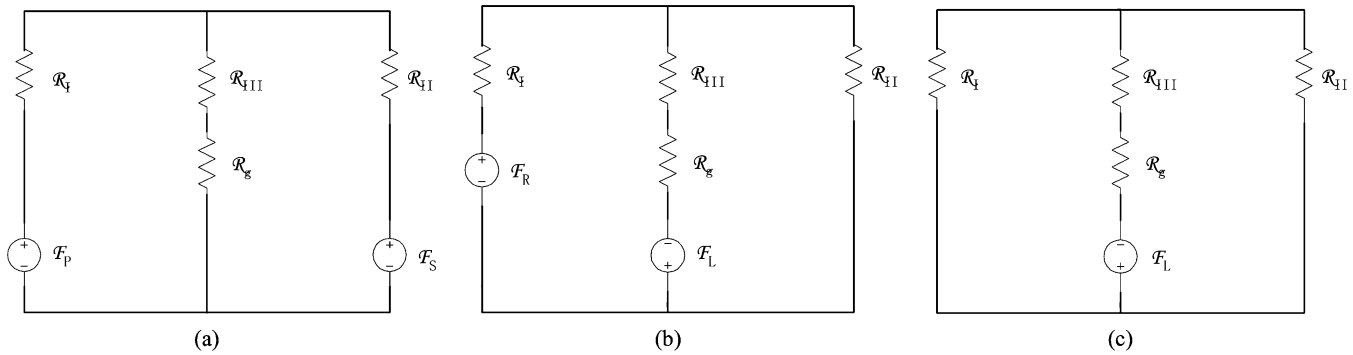

Fig. 3. State models of the forward converter in Fig. 1: (a) state 1 (Q closed), (b) state 2 (Q open, balancing mmfs between *Leg I* and *Leg II*), and (c) state 3 (Q open, mmfs of *Leg I* and *Leg II* have been balanced).

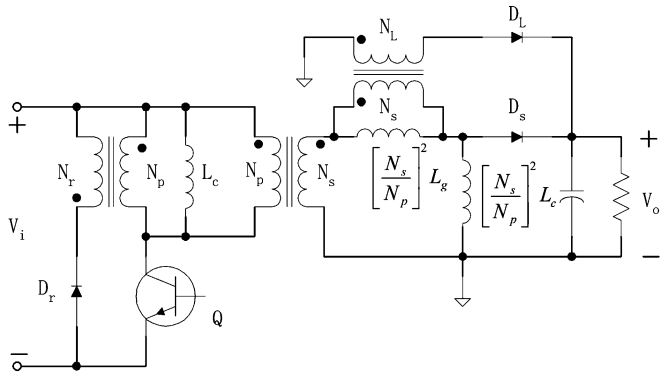

Fig. 4. Inductor model of the forward converter in Fig. 1 [2].

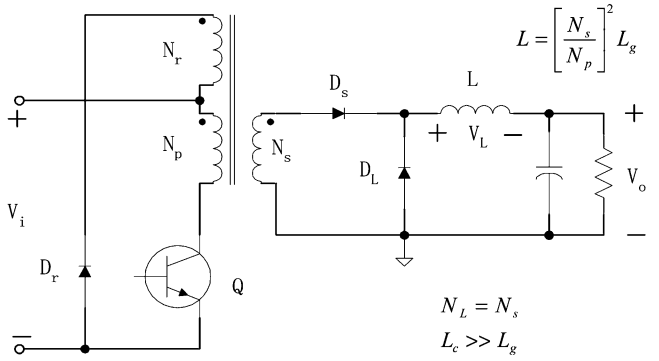

Fig. 5. Simplified inductor model of the forward converter in Fig. 1 [2].

calculation and design capabilities have not been fully explored beyond simulation.

The next section presents the revised gyrator-capacitor model that uses the gyrator relation to transform the electrical connections of windings into the magnetic circuit. Therefore, the electrical parts and all gyrators are removed. These simplifications lead to a magnetic circuit model that has similar topology to that of the reluctance model. Considering the widespread application of the reluctance model, it is reasonable to expect that the proposed modeling approach has similar potential importance. Particularly, since the proposed method makes flux rate more readily available, it provides direct access to variables necessary for proper integrated magnetic design.

III. Proposed Analysis Method by Modifying the Gyrator-Capacitor Model

A. Simplifications of the Gyrator-Capacitor Model Structure

According to the duality principle, it is possible to transform the electrical connections of windings into the magnetic circuit to create equivalent excitations to the magnetic core. The difficulty is that the electrical circuit typically includes nonlinear components, such as switching transistors and rectifiers. It is not easy to establish the concepts of their corresponding magnetic counterparts. Fortunately, in periodic steady state operation, these nonlinear components can be considered as either being turned-on or turned-off. Therefore, in a particular state, windings are actually connected to several linear components. Their magnetic equivalents can be simply created by the gyrator relation.

For example, below are several typical electrical connections of windings and their magnetic equivalents.

- When a winding is connected to a voltage source as in Fig. 7(a), a current source CS with flux rate $\dot{\Phi} = V/N$ in the magnetic circuit provides the equivalent excitation to the magnetic circuit.
- When a winding is shorted, the magnetic equivalent is an open circuit as in Fig. 7(b). This can also be derived from Fig. 7(a) with $V = 0$. It produces a current source with the current equal to zero, which is equivalent to an open circuit.
- When two winding terminals are open, the winding conducts no current but may support induced voltage. Since its mmf is zero, Fig. 7(c) shows that its magnetic equivalent is a short circuit.
- When a winding is connected across a capacitor and a resistor in parallel as in Fig. 7(d), the magnetic equivalent is the serial connection of inductance $L = N^2C$ and conductance $Z = R/N^2$. Often, in the periodic steady state analysis, the voltage on the capacitor is considered to be constant. The flux rates $\dot{\Phi}$ in inductance L can also be considered as constant. Therefore, the magnetic equivalent can be simplified to a constant current source CS.
- When two windings are in series to support a voltage source V as in Fig. 7(e), one of the flux rates, $\dot{\Phi}_a$ or $\dot{\Phi}_b$, is often determined by the outside circuit. In this case, the other flux rate can also be determined. If none of the flux rates is determined from the outside circuit, the flux rate distribution depends on the permeances of core legs and

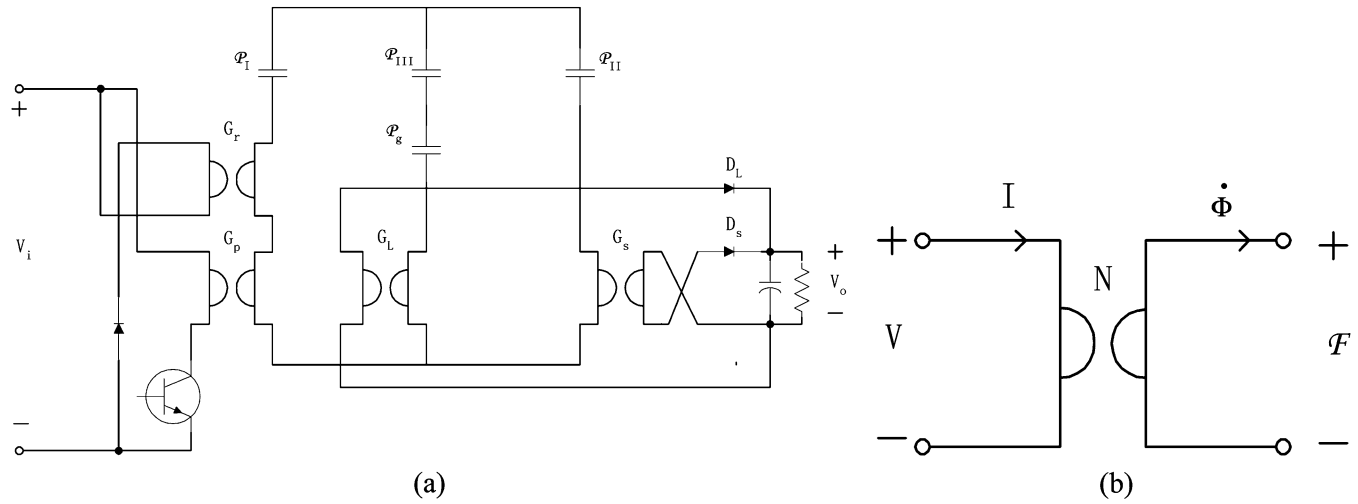

Fig. 6. Gyrator-capacitor model: (a) gyrator-capacitor model of the forward converter in Fig. 1 and (b) gyrator [12].

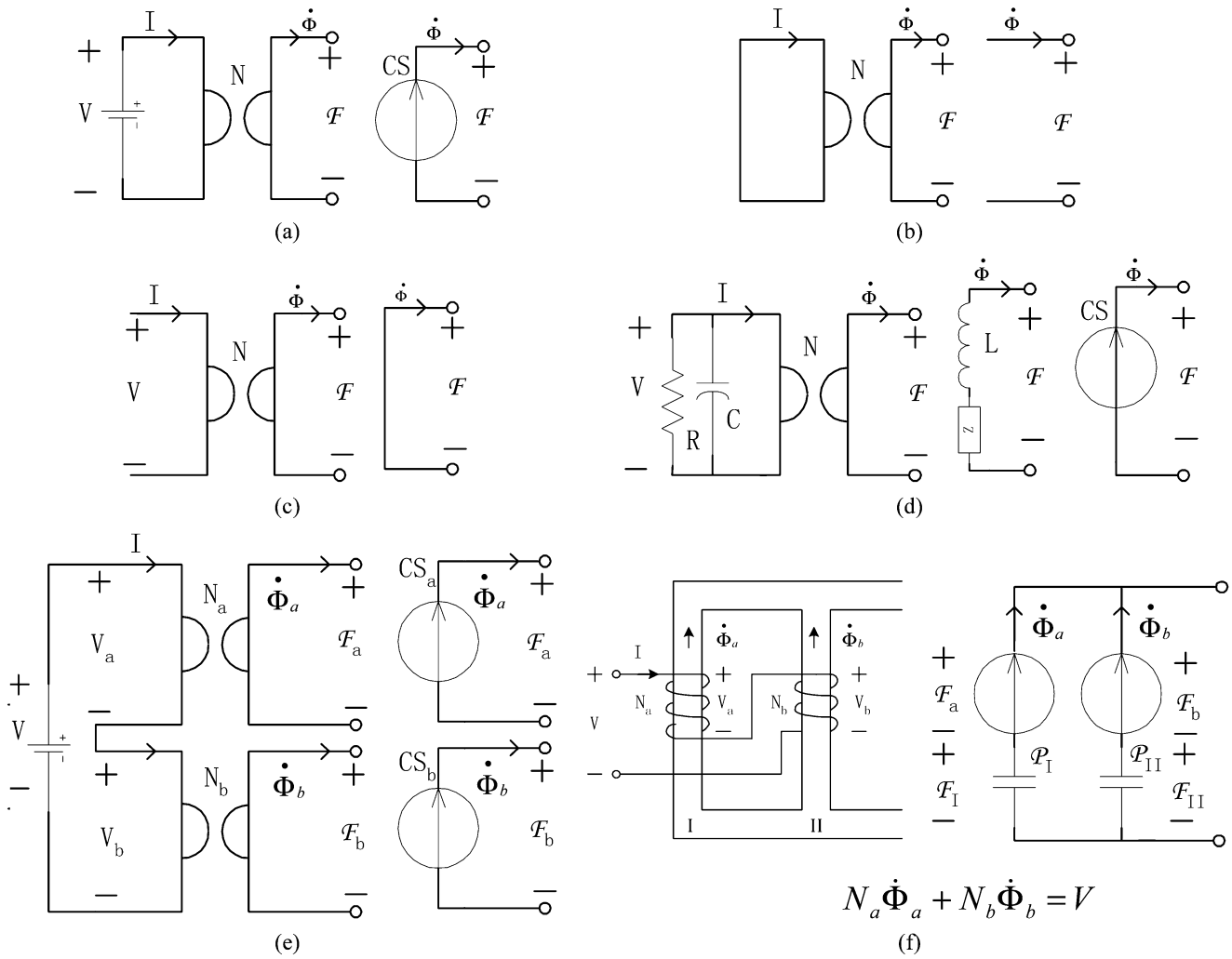

Fig. 7. Transformations from electrical circuit to magnetic circuit: (a) winding is connected to a voltage source, (b) winding is shorted, (c) winding terminals are open, (d) winding is connected across a capacitor and a resistor, (e) two windings are in serial, and (f) an example of two windings in serial.

the numbers of winding turns. For example, in Fig. 7(f), two serial connected windings are wound on two legs. Since $\mathcal{F}_a + \mathcal{F}_I = \mathcal{F}_b + \mathcal{F}_{II}$ is always valid, if $N_a = N_b$, it is easy to verify $\dot{\Phi}_a/\dot{\Phi}_b = \mathcal{P}_I/\mathcal{P}_{II}$.

Fig. 7 shows several often-used winding connections in dc/dc converters. These results can be easily proved by the gyrator relation. It is possible to find more connection types and use the gyrator relation to obtain their magnetic equivalent circuits.

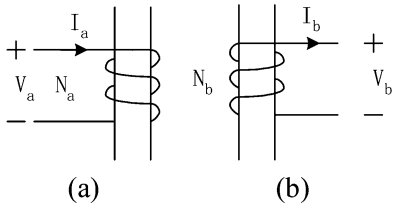

Fig. 8. Two windings for illustration of flux rate directions and mmf polarities.

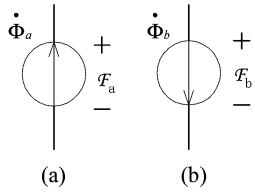

Fig. 9. (a) Flux rate direction and mmf polarity of the winding in Fig. 8(a) and (b) Flux rate direction and mmf polarity of the winding in Fig. 8(b).

Using these transformations, the periodic steady state behavior of magnetic assemblies in dc/dc converters can be easily analyzed in the proposed magnetic circuit to calculate the voltage stresses and current stresses in windings and the flux densities in core legs. More importantly, by establishing the concept of flux rates in the magnetic core, designers can integrate magnetic components more efficiently.

In these typical transformations, current sources (or current sinks) are the major excitation formats. Under the following three assumptions, the voltages applied on windings are typically constants in a particular state, which produce periodic, piecewise constant flux rate sources. The periodically constant flux rate sources make the circuit model easy to understand and analyze. The assumptions are

- the magnetic assemblies are used in PWM controlled dc/dc converters;
- the dc/dc converter regulates output voltage;
- the dc/dc converter is in periodic steady state operation.

In general, a winding can always be considered as a current source (or sink). However, if the voltage on winding is not constant in an operating state, the model may lose its design simplicity. The introduction of current source also automatically invalidates the conducting of two windings on a single core leg with two different flux rates because the serial connection of two current sources with different currents is not allowed. Thus, if two current sources in a single path are conducting simultaneously, they must have same flux rates.

The capacitor model can be created directly from the physical topology of a magnetic component and its connected electrical circuit without specifically referring to gyrators. Figs. 8 and 9 show how to determine the direction of flux rate and the polarity of mmf. The direction of the flux rate is determined by the voltage on the winding. The rule is that the voltage on the winding always tends to oppose the direction of the flux rate that is enclosed by the winding coil. Therefore, if the right hand is used to grasp the coil with fingers pointed to the negative end of the voltage, the thumb is in the direction of the flux rate. The polarity of mmf is determined by the current in the winding. The right hand is used to grasp the coil with fingers in the direction of the current. The thumb will point to the positive end of the mmf.

B. Explanation of the Capacitor Model Through an Example

Consider the circuit in Fig. 1 again. Fig. 10(a)–(c) shows its state models and Fig. 11 shows its operating waveforms. Suppose the circuit is operating in continuous current mode and the core reaches steady state mmf balance at the end of a cycle (time t_0). $\dot{\Phi}_{I\text{–}III}$ represent the reference directions of the flux rates in core legs I–III. The flux rate sources $\mathrm{CS}_p, \mathrm{CS}_s, \mathrm{CS}_r$, and CS_L show the actual directions.

Time Interval T_1, $t_0 \le t < t_1$: At time t_0, switch Q is closed. Winding N_p is connected to voltage source V_i. It generates the flux rate source CS_p, which has the value $\dot{\Phi}_I = V_i/N_p$. CS_p is the only forced excitation in this state. The flux rate flows through *Leg II* and *Leg III* as $\dot{\Phi}_{II}$ and $\dot{\Phi}_{III}$ (Note that the direction of $\dot{\Phi}_{II}$ in Fig. 10 is only for reference. The actual flux rate direction in *Leg II* is opposite to $\dot{\Phi}_{II}$.). By the rule of determining flux rate direction, the induced voltages on the other windings force diode D_s to conduct but block D_r and D_L. The flux rate sink CS_s represents the active winding N_s. Windings N_L and N_r are open. Their magnetic equivalent circuits are short circuits. $\dot{\Phi}_{II}$ is determined by the output voltage: $\dot{\Phi}_{II} = -V_o/N_s$. At the end of this state t_1, the accumulated fluxes on permeances $\mathcal{P}_{I\text{–}III}$ within time T_1 change the mmfs: $\mathcal{F}_I$ increases $V_iT_1/(N_p\mathcal{P}_I)$; $\mathcal{F}_{II}$ reduces $V_oT_1/(N_s\mathcal{P}_{II})$; $\mathcal{F}_{III}$ increases $(V_i/N_p - V_o/N_s)T_1/\mathcal{P}_{III}$.

Time Interval T_2, $t_1 \le t < t_2$: At time t_1, switch Q is open. There is no forced excitation from outside. Suppose none of the windings conducts, three core legs tend to reverse their mmf changes. To reduce $\mathcal{F}_I, \mathcal{F}_{III}$ and increases $\mathcal{F}_{II}$, the directions of the flux rates are opposite to those in time T_1. By the rule of determining flux rate direction, windings N_r and N_L conduct, which are represented by CS_r and CS_L, respectively. The magnetic core is being reset. The flux rates in three legs are $\dot{\Phi}_I = -V_i/N_r, \dot{\Phi}_{III} = -V_o/N_L, \dot{\Phi}_{II} = V_i/N_r - V_o/N_L$. Note that in Fig. 10(b), the flux rate sink CS_r supports the mmf difference between $\mathcal{F}_I$ and $\mathcal{F}_{II}$. When $\mathcal{F}_I$ and $\mathcal{F}_{II}$ are equal, CS_r will be no longer needed. Then, diode D_r is blocked and winding N_r is open. The magnetic path of *Leg I* becomes a short circuit. The circuit operation reaches the end of the state at time t_2.

Time Interval T_3, $t_2 \le t < t_3$: At time t_2, the mmfs in legs I and II have already been balanced. A third state starts for the time duration T_3 as in Fig. 10(c). In continuous current mode, the gap keeps nonzero mmf to maintain output current in N_L. The flux rate in *Leg III* is $\dot{\Phi}_{III} = V_o/N_L$. If permeances $\mathcal{P}_I$ and $\mathcal{P}_{II}$ are equal, the flux rates in *Leg I* and *Leg II* are equal: $\dot{\Phi}_I = \dot{\Phi}_{II} = V_o/(2N_L)$. The voltages induced on windings N_r and N_s are not high enough to force diodes D_s and D_r to conduct current.

IV. Differences With Reluctance Model When Calculating Magnetic Quantities

A. Discussion

The general advantages of the gyrator-capacitor model have already been presented in [9]–[13]. This section is not intended to reiterate these results. Instead, this section compares the reluctance model with the revised capacitor model when the models are used to calculate magnetic quantities. We show

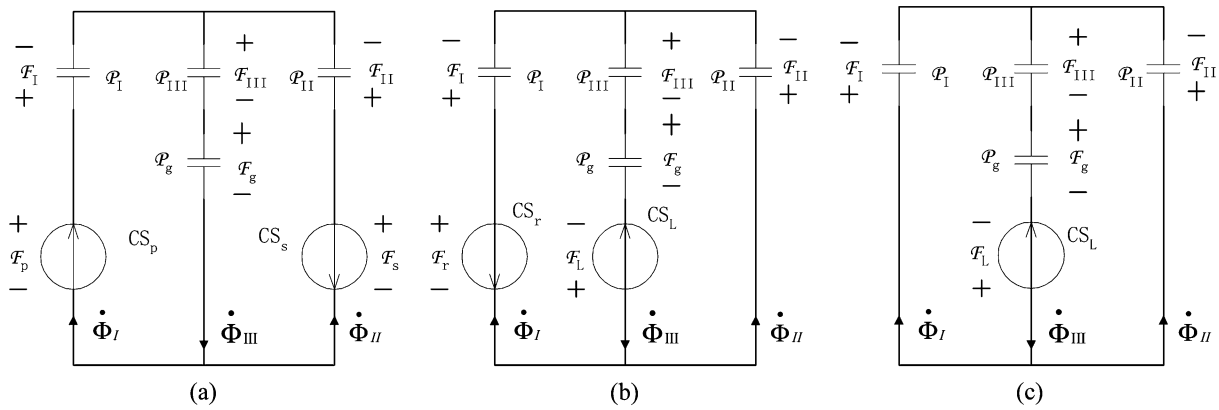

Fig. 10. Model of integrated magnetic forward converter: (a) time interval T_1, (b) time interval T_2, and (c) time interval T_3.

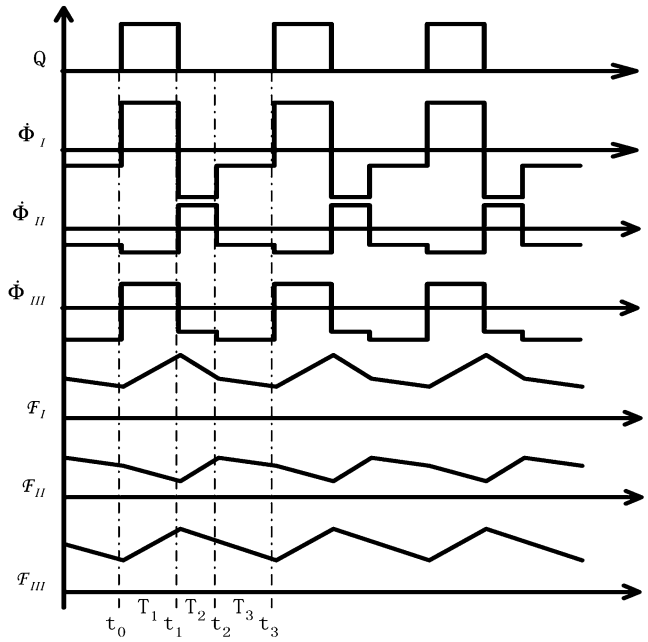

Fig. 11. Operating waveforms.

several particular design benefits that the simplified capacitor model provides regarding its new flow variable—flux rate. Table I compares the calculation procedures for several electrical and magnetic quantities.

The simplicity of calculating the voltage, the flux swing and the input-to-output voltage ratio is obvious as shown in Table I. As an example, the input-to-output voltage ratio of the circuit in Fig. 1 is derived by using the capacitor model in Fig. 10. In T_1, $\dot{\Phi}_{III} = V_i/N_p - V_o/N_s$; In T_2,$\dot{\Phi}_{III} = -V_o/N_L$; In T_3,$\dot{\Phi}_{III} = -V_o/N_L$. Further, the length of the time interval T_1 is DT and the length of time interval $T_2 + T_3$ is $(1-D)T$, where D is the duty cycle. Under steady state operation, the inductor leg should have zero flux change in each cycle. Therefore, $(V_i/N_p - V_o/N_s)DT + (-V_o/N_L)(1-D)T = 0$. This leads to $V_o/V_i = DN_LN_s/[N_p(N_s - DN_s + DN_L)]$. Often the circuit is design with $N_L = N_s$. Thus the input-to-output voltage ratio is $V_o/V_i = DN_s/N_p$. Notice that this voltage ratio is derived using the magnetic core model in Fig. 10 and does not utilize the electrical circuit model in Fig. 5. Furthermore, it is straightforward to derive an expression for V_o/V_i for the case when $N_L \neq N_s$.

Some quantities require more effort to calculate when using the capacitor model, for example, the inductor current ripple. The capacitor model does not require a derivation of an additional inductor model to calculate current ripples, but it needs to know the mmf changes on windings. If the magnetic assembly structure is simple, the reluctance model is easier because the transformation to the inductor model is quick or not necessary. Otherwise, the capacitor model shows advantages because all the calculation can be done in a single topology.

In summary, the proposed modeling approach provides benefits when there is a complicated integrated magnetic winding structure or when voltage, flux rate, flux swing are desired.

B. Example

To illustrate the magnetic design using the capacitor model, the output current ripple and peak flux density in *Leg III* of the integrated magnetic transformer in Fig. 1 are calculated. Several assumptions are made to simplify the analysis: the circuit is operating in continuous mode; all the devices are ideal; the mmfs on the permeances of the core legs $\mathcal{F}_{I-III}$ are neglected, i.e., the permeances $\mathcal{P}_{\rm I}, \mathcal{P}_{\rm II}$ and $\mathcal{P}_{\rm III}$ are assumed to be infinite compared with the permeance of the gap $\mathcal{P}_g$; also, $N_L = N_s$ [2].

1) Output Current Ripple: The output current ripple I_{o_d} can be derived from the conduction time of the inductor winding N_L. In Fig. 10(b) and (c), we have $\mathcal{F}_g = \mathcal{F}_L$. So, their ripple values are also equal: $\mathcal{F}_{g\_d} = \mathcal{F}_{L\_d}$. Within time T_2 and T_3, the flux change in the gap is $\Phi_{g\_d} = V_o(1-D)T/N_L$ $(= \dot{\Phi}_g \Delta t$, where $\Delta t = (1-D)T)$, then, $\mathcal{F}_{g\_d} = V_o(1-D)T/(N_L\mathcal{P}_g)$. By definition, $\mathcal{F}_{L\_d} = N_L I_{o\_d}$. The output current ripple is $I_{o\_d} = V_o(1-D)T/(N_L^2\mathcal{P}_g)$.

2) Peak Flux Density in Leg III: The peak flux density in *Leg III* is $B_{III\_p} = (\Phi_{g\_\rm av} + \Phi_{g\_d}/2)/A_{III}$, where A_{III} is the cross-sectional area of *Leg II*; $\Phi_{g\_\rm av}$ is the average flux bias in *Leg III*. To calculate the average flux bias, define the average output current as $I_{o\_\rm av}$. Then the average mmf on $\mathcal{P}_g$ is $I_{o\_\rm av}N_L$. So, $\Phi_{g\_\rm av} = \mathcal{P}_g I_{o\_\rm av} N_L$. Flux densities in the other legs can be calculated in a similar manner.

TABLE I
CALCULATION OF SEVERAL QUANTITIES BY THE RELUCTANCE MODEL AND THE CAPACITOR MODEL

	Reluctance Model	Capacitor Model
Voltage on winding V	If V cannot be directly obtained: 1. Transform the reluctance model to the inductor model. 2. Obtain the coupling relations to windings with known voltages. 3. Calculate V by turn ratio.	1. $V = N\dot{\Phi}$.
Input-to-output voltage ratio	1. Transform the reluctance model to the inductor model. 2. Use volt-second balance on the (equivalent) inductor.	1. Use flux change balance on permeance.
Current ripple ΔI in winding	1. Transform the reluctance model to the inductor model. 2. Obtain the equivalent inductance L in the desired current path. 3. The voltage on L within time duration Δt can be expressed as $V_L = L\Delta I/\Delta t$.	1. Derive flux swing on permeance $\Delta\Phi = \int\dot{\Phi}dt$. 2. Derive mmf swing on permeance $\Delta\mathcal{F}_c = \Delta\Phi/\mathcal{P}$. 3. Derive mmf swing of winding $\Delta\mathcal{F}_w$ by using KVL and KCL. 4. If the number of winding turns is N, $\Delta I = \Delta\mathcal{F}_w/N$.
Average flux Φ	1. Derive average mmf on winding $\mathcal{F}_w = NI$. 2. Derive average mmf on permeance $\mathcal{F}_c$ by using KVL and KCL. 3. $\Phi = \mathcal{F}_c/\mathcal{R}$.	1. Derive average mmf on winding $\mathcal{F}_w = NI$. 2. Derive average mmf on permeance $\mathcal{F}_c$ by using KVL and KCL. 3. $\Phi = \mathcal{F}_c\mathcal{P}$.
Flux swing $\Delta\Phi$	1. For leg with windings, use $\Delta\Phi = \Delta\mathcal{F}_w/\mathcal{R}$, where $\Delta\mathcal{F}_w = N\Delta I$. 2. For leg without windings, use KVL and KCL to derive $\Delta\Phi$ in the circuit model.	1. $\Delta\Phi = \int\dot{\Phi}dt$.

V. MAGNETIC INTEGRATION

The major difference between an integrated magnetic component and a discrete magnetic component is that the integrated magnetic component contains more than one major flux path. So, magnetic integration can be viewed as combining two or more flux paths in separated cores into one magnetic assembly. Three types of magnetic integration techniques have been discussed in [1]–[3], [17] and are summarized as follows.

Type 1: If the flux rates in two or more flux paths are identical, these flux paths can be integrated together. A well-known example is the coupled inductors in multiple-output dc/dc converters.

Type 2: If the flux rates in two or more flux paths are linearly related, these flux paths can be combined into one core as separate legs. An example is shown later.

Type 3: If the flux rates in two or more flux paths are not related, these flux paths can be combined into one core with an additional leg that provides an extra flux path for the difference of the flux rates.

The three types of integration techniques are inevitably based on flux rate (sometimes referred to as "ac flux" [17] or "the rate of flux change" [3]). Since in the capacitor model, the flux rate is readily available, it is reasonable to expect that the capacitor model makes the magnetic integration more convenient and direct.

To compare the two models when the models are used to integrated magnetic components, the next example shows the procedures by usage of the reluctance model [17] and the capacitor model. In this example, three magnetic cores in a current doubler circuit are combined into one magnetic assembly. Fig. 12 shows a current doubler circuit. Fig. 12 is the schematic including transformer T and two inductors L_1, L_2. Fig. 13 implements the three magnetic components on "C" shape cores.

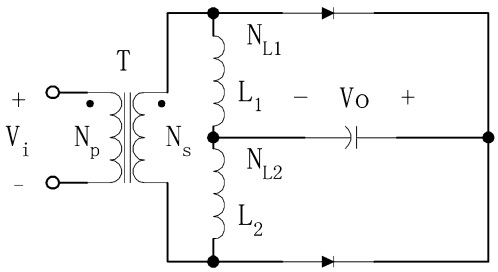

Fig. 12. Schematic of a current doubler circuit.

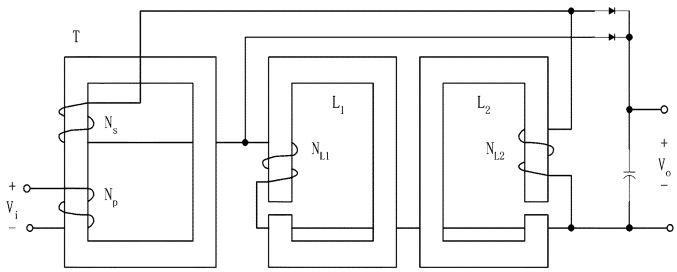

Fig. 13. Circuit implementation with "C" shape cores.

A. Magnetic Integration Using the Reluctance Method [17]

This method represents the equivalent inductance for each winding in term of reluctance. These expressions are then investigated to configure an appropriate core-winding structure. To derive the inductance, in Fig. 14(a), suppose a current i_p is injected into Port a-b. The inductance looking into Port a-b is $L_{ab} = L_m//[(N_p/N_s)^2L_1 + (N_p/N_s)^2L_2]$, where $L_m = N_p^2/\mathcal{R}_c, L_1 = N_{L1}^2/\mathcal{R}_1, L_2 = N_{L2}^2/\mathcal{R}_2; \mathcal{R}_c, \mathcal{R}_1$, and $\mathcal{R}_2$ are the reluctances of the magnetic cores in T, L_1,

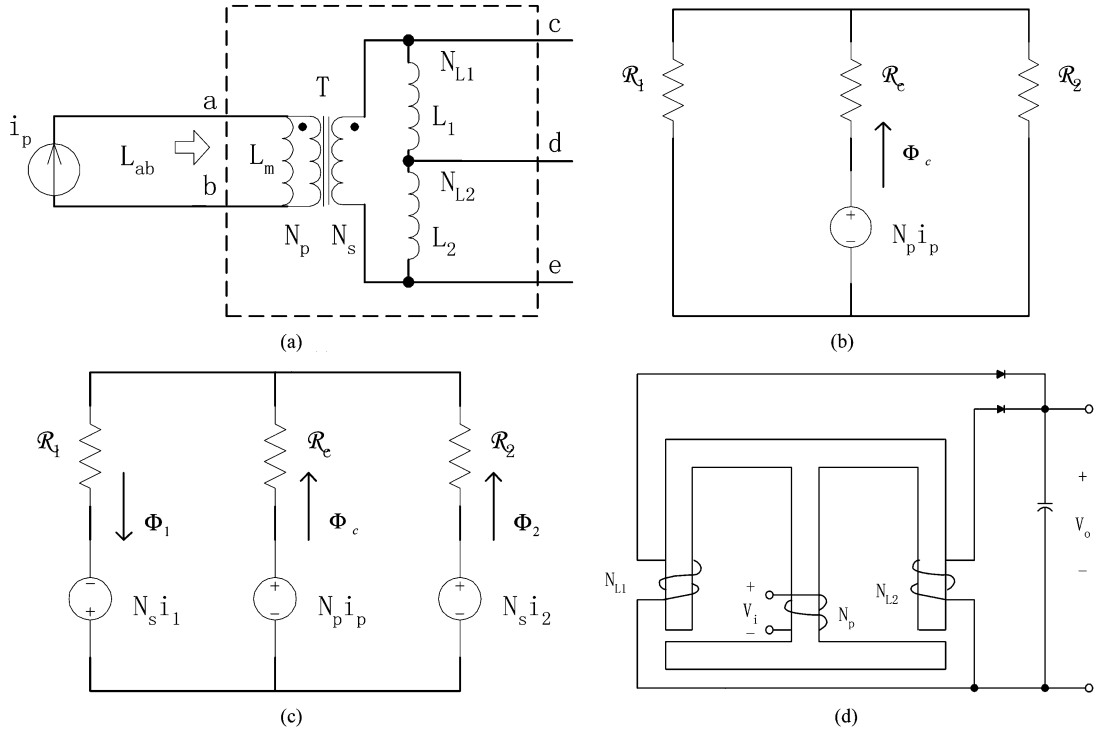

Fig. 14. Magnetic integration using the reluctance model [17].

TABLE II
FLUX RATES IN THREE MAGNETIC CORES

	$\dot{\Phi}_T$	$\dot{\Phi}_{L1}$	$\dot{\Phi}_{L2}$
$V_i > 0$	$\frac{V_i}{N_p}$	$-\frac{V_o}{N_{L1}}$	$\frac{V_o}{N_{L2}} - \frac{V_i N_s}{N_p N_{L2}}$
$V_i = 0$	0	$-\frac{V_o}{N_{L1}}$	$\frac{V_o}{N_{L2}}$
$V_i < 0$	$-\frac{V_i}{N_p}$	$\frac{V_i N_s}{N_p N_{L1}} - \frac{V_o}{N_{L1}}$	$\frac{V_o}{N_{L2}}$

and L_2. Let $N_s = N_{L1} = N_{L2}$. Then the inductance $L_{ab} = N_p^2/(\mathcal{R}_c + \mathcal{R}_1//\mathcal{R}_2)$. Suppose Φ_c is the flux enclosed by winding N_p. By definition, $L_{ab} = N_p\Phi_c/i_p$. Therefore, $\Phi_c = N_p i_p/(\mathcal{R}_c + \mathcal{R}_1//\mathcal{R}_2)$.

The expression for Φ_c can be translated into the reluctance model of Fig. 14(b). Applying the same method to derive the inductance looking into Port c-d and Port d-e, then using the superposition theory, a complete reluctance model can be obtained as in Fig. 14(c). Corresponding to this reluctance model, its physical implementation can be configured as Fig. 14(d). This is an integrated magnetic version of the current doubler circuit in Fig. 13. Notice that the reluctance model cannot serve the integration independently. The topology derivation relies on the interpretation of the inductance for each port in terms of the reluctance. This model well explains the coupling between windings. However, it does not give direct indications of the physical transitions of the magnetic cores and the removal of winding N_s.

B. Magnetic Integration Using the Capacitor Method

The capacitor models for three operating states are drawn in Fig. 15(a). Table II shows the flux rates in the three flux paths. Assume $N_s = N_{L1} = N_{L2}$. Obviously, in any state, we have $\dot{\Phi}_T + \dot{\Phi}_{L1} + \dot{\Phi}_{L2} = 0$. The flux rates in the three flux paths satisfy the Type 2 integration rule. Therefore, three flux paths can be integrated into one core with separate legs. The combined model in each state is shown in Fig. 15(b), and the integrated magnetic assembly is shown in Fig. 15(d) [18]. Notice that the circuit model in Fig. 15(b) always maintains $\dot{\Phi}_T + \dot{\Phi}_{L1} + \dot{\Phi}_{L2} = 0$ by KCL. Therefore, it is a valid integration of the magnetic assemblies in Fig. 13.

Fig. 15(d) is not the only integrated magnetic format of the current doubler circuit in Fig. 13. Since the magnetic integration does not change the flux rates in the original flux paths, Table II is valid for the magnetic assembly in Fig. 15(d) under the assumption $N_s = N_{L1} = N_{L2}$. With assumption $N_s = N_{L1} = N_{L2}$, Table II also indicates that when $V_i > 0$, independent flux rates $\dot{\Phi}_T$ and $\dot{\Phi}_{L1}$ are determined by winding N_p and winding N_{L1}; when $V_i = 0$, independent flux rates $\dot{\Phi}_{L1}$ and $\dot{\Phi}_{L2}$ are determined by winding N_{L1} and winding N_{L2}; when $V_i < 0$, independent flux rates $\dot{\Phi}_T$ and $\dot{\Phi}_{L2}$ are determined by winding N_p and winding N_{L2}. Winding N_s makes no contribution to the definition of any flux rate in the core. So, the circuit model in Fig. 15(b) can maintain the same flux rate even without winding N_s. This leads to the same integrated magnetic circuit as in Fig. 14(d). Its capacitor model is drawn in Fig. 15(c). Flux rate sources CS_{L2} and CS_{L1} are removed in states $V_i > 0$ and $V_i < 0$ respectively because by the rule of determining flux rate direction, windings N_{L2} and N_{L1} do not conduct current without winding N_s. The models in Fig. 15(c) maintain the same $\dot{\Phi}_T$, $\dot{\Phi}_{L1}$, and $\dot{\Phi}_{L2}$, despite the fact that the secondary winding N_s is removed. Therefore, it is also a valid integrated magnetic

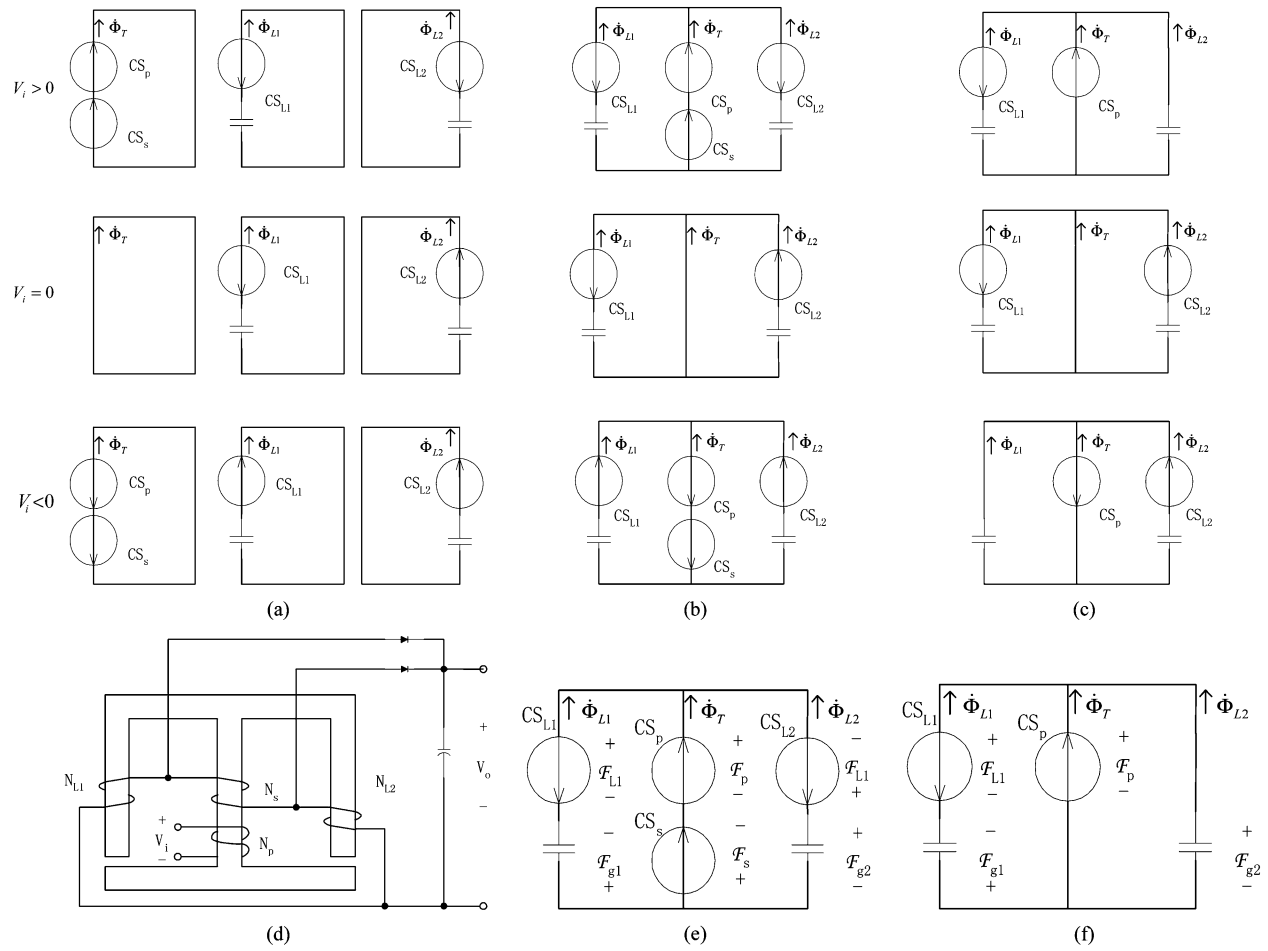

Fig. 15. Magnetic integration using the capacitor model: (a) capacitor model of discrete cores, (b) capacitor model of combined core, (c) eliminate redundant current source in (b), (d) implementation of (b), (e) detailed model of (b) for $V_i > 0$, and (f) detailed model of (c) for $V_i > 0$.

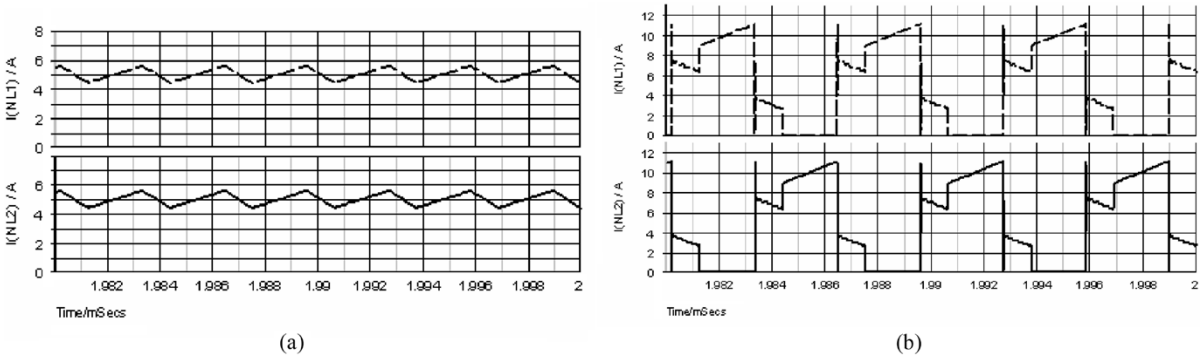

Fig. 16. Simulation results to show the winding current difference between the circuits in Figs. 14(d) and 15(d): (a) currents in winding N_{L1} and N_{L2} of circuit in Fig. 15(d) and (b) currents in winding N_{L1} and N_{L2} of circuit in Fig. 14(d).

implementation of the circuit in Fig. 13. (Further development of integrated magnetic current doubler circuit can be referred to [19], [20].) However, the removal of winding N_s changes the mmf distribution in the core. The currents in the windings are expected to be different from the original circuit. If the reader is interested in learning more about magnetic integration synthesis rules using the capacitor modeling approach, they can be found in [21] in more detail.

It is interesting to see how the winding currents change with and without winding N_s. Fig. 15(e) and (f) shows the detailed models of the circuits in Figs. 15(d) and 14(d) for state $V_i > 0$, respectively. In the circuit of Fig. 15(d), since $\mathcal{F}_p = \mathcal{F}_s$ is valid for all three states, $\mathcal{F}_{L1} \equiv \mathcal{F}_{g1}$. It is known that the mmf on the permeance is smooth. So, the current in winding N_{L1} is expected to be smooth. On the other hand, in Fig. 15(f), $\mathcal{F}_{L1} = \mathcal{F}_{g1} + \mathcal{F}_p$. When $V_i = 0$, we have $\mathcal{F}_p = 0$. $\mathcal{F}_{L1}$ is then equal to

$\mathcal{F}_{g1}$ only. The current in winding N_{L1} is not smooth. Furthermore, without winding N_s, winding N_{L2} does not conduct when $V_i > 0$. So the currents in the inductor windings are even discontinuous. The integrated magnetic circuit in Fig. 14(d) simplifies the transformer structure by removing winding N_s with the penalty of distorted inductor winding currents.

As an instructive illustration, Fig. 16 shows the simulation results of a dc/dc converter with: input voltage 48 V; output voltage 5 V; output power 50 W; $N_p = 12; N_s = N_{L1} = N_{L2} = 4$. The permeances of the gaps are equal to 330 nH. The currents in windings N_{L1} and N_{L2} verify the above results.

In summary, both the reluctance model and the capacitor model can be used to integrate magnetic components. The integration in the reluctance model is based on the mathematical derivation of flux, reluctance and inductance. It is better than the capacitor model to interpret the coupling between windings. The integration in the capacitor model is based on the flux rates and winding movement techniques. Therefore, it can be used to directly manipulate the physical core structure and windings. It is easier to obtain multiple topologies by structure transitions, and, thus, bring intuition for magnetic integration.

VI. Conclusion

This paper shows that the capacitor model is a simple and effective analysis method for integrated magnetic components. Under certain assumptions, this modeling approach is extended by replacing gyrators with current sources and short or open circuit to symbolize the electrical actions on windings. The revised model is suitable for conceptual magnetic design and integration. Several applications in magnetic design and magnetic integration illustrate the usage of this approach. Its advantages over the conventional reluctance model in integrated magnetic design are described.

References

[1] E. Bloom, "New integrated-magnetic dc–dc power converter circuits and systems," in *Proc. IEEE APEC*, 1987, pp. 57–66.

[2] ——, "Core selection for & design aspects of an integrated-magnetic forward converter," in *Proc. IEEE APEC*, 1986, pp. 141–150.

[3] R. Severns and E. Bloom, *Modern DC/DC Switchmode Power Converter Circuits*. New York: Van Nostrand Reinhold Company, Dec. 1985.

[4] G. W. Ludwig and S. El-Hamamsy, "Coupled inductance and reluctance models of magnetic components," *IEEE Trans. Power Electron.*, vol. 6, no. 2, pp. 240–250, Apr. 1991.

[5] A. F. Witulski, "Modeling and design of transformers and coupled inductors," in *Proc. IEEE APEC*, 1993, pp. 589–595.

[6] ——, "Introduction to modeling of transformers and coupled inductors," *IEEE Trans. Power Electron.*, vol. 10, no. 3, pp. 349–357, May 1995.

[7] S. El-Hamamsy and E. I. Chang, "Magnetics modeling for computer-aided design of power electronics circuits," in *Proc. IEEE PESC*, 1989, pp. 635–645.

[8] P. L. Wong, F. C. Lee, X. Jia, and W. D. Van, "A novel modeling concept for multi-coupling core structures," in *Proc. IEEE APEC*, 2001, pp. 102–108.

[9] R. Buntenbach, "Improved circuit models for inductors wound on dissipative magnetic cores," in *Proc. 2nd Asilomar Conf. Circuits Systems*, Pacific Grove, CA, Oct. 1968, pp. 229–236.

[10] ——, "A comprehensive circuit model for the electromechanical/acoustic transducer," *IEEE Trans. Audio Electroacoust.*, vol. 19, no. 3, pp. 249–252, Sep. 1971.

[11] ——, "A generalized circuit model for multiwinding inductive devices," *IEEE Trans. Magnetics*, vol. MAG-6, no. 1, pp. 65–65, Mar. 1970.

[12] D. C. Hamill, "Lumped equivalent circuits of magnetic components: The gyrator-capacitor approach," *IEEE Trans. Power Electron.*, vol. 8, no. 2, pp. 97–103, Apr. 1993.

[13] ——, "Gyrator-capacitor modeling: A better way of understanding magnetic components," in *Proc. IEEE APEC*, 1994, pp. 326–332.

[14] D. K. Cheng, L. Wong, and Y. S. Lee, "Design, modeling, and analysis of integrated magnetics for power converters," in *Proc. IEEE PESC*, 2000, pp. 320–325.

[15] M. E. Eaton, "Adding flux paths to SPICE's analytical capability improves the ease and accuracy of simulating power circuits," in *Proc. IEEE APEC*, 1998, pp. 386–392.

[16] P. G. Blanken, "A lumped winding model for use in transformer models for circuit simulation," *IEEE Trans. Power Electron.*, vol. 16, no. 3, pp. 445–460, May 2001.

[17] W. Chen, "Low voltage high current power conversion with integrated magnetic," Ph.D. dissertion, Virginia Polytech. Electron. Ctr. (VPEC), Blacksburg, Apr. 27, 1998.

[18] O. S. Seiersen, "Power Supply Circuit with Integrated Magnetic Components," U.S. Patent 5 335 163, Aug. 2, 1994.

[19] G. Q. Morris, "Magnetically integrated full wave dc to dc converter," U.S. Patent 5 555 494, Sep. 10, 1996.

[20] P. Xu, Q. Wu, P. Wong, and F. C. Lee, "A novel integrated current doubler rectifier," in *Proc. IEEE APEC*, 2000, pp. 735–740.

[21] L. Yan and B. Lehman, "Better understanding and synthesis of integrated magnetics with simplified gyrator model method," in *Proc. IEEE APEC*, 2001, pp. 433–438.

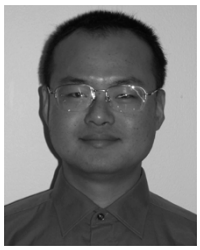

Liang Yan (M'04) received the B.E. and M.E. degrees from Shanghai Jiaotong University, Shanghai, China, in 1995 and 1998, respectively, and Ph.D. degree in electrical engineering from Northeastern University, Boston, MA, in 2004.

From 1998 to 1999, he worked for Huawei Electrical Inc., Shenzhen, China. He is currently working for MKS ENI products in Rochester, NY.

Brad Lehman (M'95) received the B.S. degree from the Georgia Institute of Technology, Atlanta, in 1987, the M.S. degree from the University of Illinois at Champaign-Urbana, in 1988, and the Ph.D. degree from the Georgia Institute of Technology, Atlanta, in 1992, all in electrical engineering.

He is presently an Associate Professor in the Department of Electrical and Computer Engineering, Northeastern University, Boston, MA, and previously was a Hearin Hess Distinguished Assistant Professor at Mississippi State University. He was previously an NSF Presidential Faculty Fellow and a Visiting Scientist at the Massachusetts Institute of Technology, Cambridge. He performs research in the areas of power electronics, electric motor drives, and control. A primary focus of his research is in the modeling, design and control of dc–dc converters.

Dr. Lehman received the Alcoa Science Foundation Fellowship. He serves as an Associate Editor of the IEEE Transactions on Power Electronics, and, from 1993 to 1997, served as an Associate Editor for the IEEE Transactions on Automatic Control.